



## 1 Nitrous oxide as second most important greenhouse gas in tropical peatlands

2  
3 Jaan Pärn<sup>1</sup>, Mikk Espenberg<sup>1</sup>, Kaido Soosaar<sup>1</sup>, Kuno Kasak<sup>1</sup>, Sandeep Thayamkottu<sup>1</sup>, Thomas  
4 Schindler<sup>1,2</sup>, Reti Ranniku<sup>1</sup>, Kristina Sohar<sup>1</sup>, Lizardo Fachín Malaverri<sup>3</sup>, Lulie Melling<sup>4</sup>, Ülo  
5 Mander<sup>1</sup>

6 <sup>1</sup> Institute of Ecology and Earth Sciences, University of Tartu, Estonia (jaan.parn@ut.ee)

7 <sup>2</sup> Department of Ecosystem Trace Gas Exchange, Global Change Research Institute of the Czech Academy of  
8 Sciences, Brno, Czech Republic

9 <sup>3</sup> Peruvian Amazon Research Institute (IIAP), Iquitos, Peru

10 <sup>4</sup> Sarawak Tropical Peat Research Institute, Sarawak, Malaysia

11 *Correspondence to:* Jaan Pärn (jaan.parn@ut.ee)

## 12 Abstract

13 Earth's climate largely depends on carbon and nitrogen exchange between the atmosphere and  
14 tropical peatland ecosystems. Permanently wet peatlands take up carbon dioxide in plants and  
15 accumulate organic carbon in soil but release methane. Man-made drainage releases carbon  
16 dioxide from peat soils. Carbon and nitrous gas exchange and their relationships with tropical  
17 peatland conditions are poorly understood. We analysed natural peat swamp forests and fens,  
18 moderately drained and dry peatlands under a wide variety of land uses. The tropical peat  
19 swamp forests were large greenhouse gas sinks while tropical peatlands under moderate and  
20 low soil moisture levels emitted carbon dioxide and nitrous oxide. Carbon dioxide uptake of  
21  $160 \text{ mg m}^{-2} \text{ h}^{-1}$  dominated the net greenhouse gas budgets overall, while nitrous oxide emission  
22 of  $90 \text{ mg CO}_2\text{-equivalent m}^{-2} \text{ h}^{-1}$  on average was the second most important contributor (ahead  
23 of average methane emissions of  $36 \text{ mg CO}_2\text{-equivalent m}^{-2} \text{ h}^{-1}$ ) across the whole tropical peat  
24 moisture range.

## 26 1 Introduction

27 Peatlands function as a substantial reservoir of carbon (C) and nitrogen (N) (Leifeld and  
28 Menichetti, 2018, Loisel et al., 2021). In undisturbed conditions, specifically within  
29 permanently waterlogged peat swamp forests, C accumulates in the peat over extended periods,  
30 spanning tens of thousands of years (Melling et al., 2005a; Ruwaimana et al., 2020). Natural  
31 and anthropogenic disturbances have the potential to release stored C and N as greenhouse  
32 gases (GHG). This potential is particularly high in tropical peatlands (IPCC, 2021). Drought,  
33 an increasingly prevalent ecological change in tropical zones, accelerates ecosystem alterations  
34 by shortening the growth period (IPCC, 2021), and elevating ecosystem respiration (ER)  
35 (Karhu et al., 2014; Jassej et al., 2021). In dry seasons, ecosystem respiration may surpass  
36 gross primary production (GPP) by an average of  $600 \text{ mg C day}^{-1}$ , even when the soil is still  
37 wet (Griffis et al., 2020; Pärn et al., 2023). We are still short of fully understanding the total  
38 effect of soil-moisture variations on C balances in low-latitude peatlands, necessitating further  
39 research efforts (Zhou et al., 2023).

40 The anoxic decomposition of peat in conditions of a high water table results in the production  
41 of methane ( $\text{CH}_4$ ) (Melling et al., 2005b; Teh et al., 2017; Hergoualc'h et al., 2020).  $\text{CH}_4$  is a  
42 potent greenhouse gas, exhibiting a global warming potential equivalent to 28 times that of  
43 carbon dioxide ( $\text{CO}_2$ ) (IPCC, 2021). The  $\text{CH}_4$  generated within a peat layer escapes to the  
44 topsoil, where it may be either consumed by methanotrophs or be emitted. The latter can  
45 happen either directly through the peat or facilitated through plant conduits (Soosaar et al.,  
46 2022). As a result, the hydroclimate, biogeochemistry of distinct peat layers, as well as the type  
47 of vegetation and land use, emerge as potential influencing factors for  $\text{CH}_4$  emissions in  
48 tropical peatlands.



49 Suboxic processes occurring within N-rich peat under moderate water content (50 to 60%) lead  
50 to the production of nitrous oxide (N<sub>2</sub>O) (Melillo et al., 2001; Jauhiainen et al., 2012; Rubol et  
51 al., 2012; Hu et al., 2015; Pärn et al., 2018; Hergoualc’h et al., 2020; Pärn et al., 2023).  
52 Globally, regions such as the Amazon rainforest, Congo, and Southeast Asia exhibit the highest  
53 N<sub>2</sub>O emissions (Ricaud et al., 2009). Amazonia alone yields 1,300 Gg N<sub>2</sub>O-N yr<sup>-1</sup> (Melillo et  
54 al., 2001). The conversion of peatlands for agriculture, particularly in Southeast Asia, produces  
55 huge amounts of N<sub>2</sub>O (Hadi et al., 2000; Melling et al., 2007). Brazil, due to increased  
56 fertilization, is also a major contributor to the global rise in N<sub>2</sub>O emissions (Thompson et al.,  
57 2019). The role of peatlands in the total tropical N<sub>2</sub>O emissions remains poorly understood  
58 (van Lent et al., 2015; Guilhen et al., 2020). Peat swamps in Peru and Southeast Asia exhibit  
59 varying N<sub>2</sub>O emissions, with a Peruvian palm peat swamp producing 0.5 to 2.6 kg N<sub>2</sub>O-N ha<sup>-1</sup>  
60 yr<sup>-1</sup> and Southeast Asian peat swamp forests producing 2.7 ± 1.7 kg N<sub>2</sub>O-N ha<sup>-1</sup> yr<sup>-1</sup> (average  
61 ± standard deviation; van Lent et al., 2015). However, the sources of N<sub>2</sub>O (nitrate (NO<sub>3</sub><sup>-</sup>) or  
62 ammonium (NH<sub>4</sub><sup>+</sup>)) and their susceptibility to climatic changes, such as water table, oxygen  
63 (O<sub>2</sub>), and temperature fluctuations, remain unclear. Studies on mineral soil are deemed  
64 unreliable for comprehending the impact of climate change on peatlands due to their  
65 fundamentally different biogeochemistry (Rydin and Jeglum, 2013). Where undrained,  
66 peatlands are water-saturated throughout the year, shielding the C and N stocks (Turetsky et  
67 al., 2015). However, deforestation, often with fire, jeopardizes the C and N stocks (Turetsky et  
68 al., 2015; Lilleskov et al., 2019; Swails et al., in press).  
69 Limited studies have compared greenhouse gas fluxes across different land uses and water  
70 regimes in tropical peatlands. Here, we analyse GHG exchange based on field chamber  
71 measurements of ER, N<sub>2</sub>O and CH<sub>4</sub> fluxes (Pärn et al., 2018, 2023 and unpublished) and  
72 satellite data of gross primary production (GPP) in 12 tropical peatlands in South America,  
73 Africa and Southeast Asia during the wet and dry seasons. We further investigate explanatory  
74 factors of the GHG fluxes mostly focusing on drainage, soil temperature and soil chemistry.

## 75 **2 Methods**

### 76 **2.1 Field sampling**

77 We conducted a survey of CO<sub>2</sub>, CH<sub>4</sub> and N<sub>2</sub>O fluxes and potentially controlling environmental  
78 variables at peatland sites in the Peruvian Amazon, French Guiana, Uganda, Burma, and the  
79 Malaysian Borneo states of Sarawak and Sabah during both the dry season (i.e. annual water  
80 table minimum) and rainy period (annual water table maximum) of each site between 2013 and  
81 2022. We selected a total of 12 forested, fen, grassland, arable and oil palm plantation sites  
82 (Fig. 1) in the rainy tropical (A) climate zones of the Köppen classification from our global  
83 wetland soil database (Pärn et al., 2018, 2023 and unpublished; Fig. 1). The hydrology and  
84 trophic status of the natural sites ranged from groundwater-fed swamps and fens to rain-fed  
85 peat swamp forests. We also selected the sites to represent the full typical range of land uses  
86 of the rainy tropical belt. Accordingly, our study sites represent peatlands that have been arable  
87 for >5 years (Borneo, Burma, Peru and Uganda), intensively (more than once a year) grazed  
88 peat meadows (Uganda), and drained fens (Guiana (Espenberg et al., 2018) and Burma),  
89 swamp forests (Peru, Sabah and Sarawak) and fens (Espenberg et al., 2018) under no direct  
90 human influence in each study region. To capture the full variety of GHG fluxes at a site, we  
91 set up transects of 2–3 plots, each containing 3–4 opaque chambers, arranged along 25–100 m  
92 of terrain. We sampled gas from the chambers during 3–6-day campaigns. We measured ER  
93 (in mg CO<sub>2</sub> m<sup>-2</sup> h<sup>-1</sup>), CH<sub>4</sub> and N<sub>2</sub>O fluxes (both in mg m<sup>-2</sup> h<sup>-1</sup>) from the samples using a gas  
94 chromatograph (Pärn et al., 2018; Bahram, Espenberg, Pärn et al., 2022). We collected soil  
95 samples of 150–200 g from the chambers at 0–10 cm depth after the final gas sampling, and  
96 transported them to laboratories in Tartu, Estonia.



97



98

99 Fig. 1. Location of peatland study sites. Each location contains a natural peatland and an  
100 equivalent peatland under direct human impact. Data from Pärn et al. (2018, 2023 and partly  
101 unpublished (Sarawak)). Global peatland map: Leifeld and Menichetti (2018).

## 102 2.2 Estimation of GPP

103 As an estimate of GPP, we used MOD17A2H V006 data (Running et al., 2015) developed from  
104 the MODIS sensor onboard the Terra and Aqua remote sensing satellites and expressed in mg  
105 CO<sub>2</sub> m<sup>-2</sup> h<sup>-1</sup>. MOD17A2H V006 is based on the radiation use efficiency concept (Monteith,  
106 1972) with three major components. The first assumption is that GPP is directly related to the  
107 solar energy absorbed by plants. Second, the concept assumes a connection between absorbed  
108 solar energy and satellite-derived spectral indices such as NDVI. The third assumption is that  
109 for biophysical reasons, the actual conversion efficiency of absorbed solar energy is lower than  
110 the theoretical value. The calculation of GPP (Equation 1) requires radiation use efficiency and  
111 absorbed photosynthetically active radiation (APAR) measurements. APAR calculates the  
112 available leaf area index (LAI) to absorb incident solar energy. This estimate is then converted  
113 into GPP by multiplying APAR with radiation use efficiency ( $\epsilon$ ) (Equations 1 and 2). Remote  
114 sensing data usually provide the fraction of photosynthetically active radiation (FPAR;  
115 Equation 3). APAR can be calculated by Equation 4 (Sellers, 1987). This requires estimation  
116 of incidental photosynthetically active radiation (IPAR) (Equation 5), which is extracted from  
117 the GMAO/NASA dataset (Running et al., 2015).

$$118 \text{GPP} = \epsilon * \text{APAR} \quad (1)$$

$$119 \epsilon = \epsilon_{\max} * T_{\min\_scalar} * \text{VPD\_scalar} \quad (2)$$

$$120 \text{FPAR} = \text{APAR} / \text{PAR} \approx \text{NDVI} \quad (3)$$

$$121 \text{APAR} = \text{IPAR} * \text{FPAR} \quad (4)$$

$$122 \text{IPAR} = \text{SWR}_{\text{rad}} * 0.45 \quad (5)$$

123  $\epsilon_{\max}$  is the maximum radiation conversion efficiency in kg C MJ<sup>-1</sup> which is obtained from the  
124 Biome Properties Look-Up Table (BPLUT) of the at-launch land cover product of MODIS  
125 (MOD12; Friedl and Sulla-Menashe, 2020).

126  $T_{\min\_scalar}$  and  $\text{VPD\_scalar}$  are the ramp functions of  $T_{\min}$  and VPD. This calculation requires the  
127 following parameters extractable from the GMAO/NASA dataset (Running et al., 2015):

128  $T_{\min\_max}$  (°C) – the daily minimum temperature at which  $\epsilon = \epsilon_{\max}$  for an optimal VPD

129  $T_{\min\_min}$  (°C) – the daily minimum temperature at which  $\epsilon = 0$  at any VPD

130  $\text{VPD}_{\max}$  (Pa) – the daylight average vapor pressure deficit at which  $\epsilon = \epsilon_{\max}$  for an optimal  $T_{\min}$

131  $\text{VPD}_{\min}$  (Pa) – the daylight average vapor pressure deficit at which  $\epsilon = 0.0$  at any  $T_{\min}$

132  $\text{SWR}_{\text{rad}}$  = Incident shortwave radiation used for calculating IPAR.

133 We extracted GPP values for our sites from the dataset (kg C m<sup>-2</sup> 8 days<sup>-1</sup>) for the ground  
134 measurement dates and expressed the values in mg C m<sup>-2</sup> h<sup>-1</sup>.

135 A >50% underestimate of the negative effect of drought on the MODIS GPP product has been  
136 suspected (Stocker et al., 2019). We tested the significance of this possible underestimate by  
137 multiplying the GHG exchange values from our dry (<0.4 m<sup>3</sup> m<sup>-3</sup> SWC) by a factor of 0.5 and  
138 using them in the regression analyses. The patterns of GHG exchange values vs. SWC after  
139 this reduction became less pronounced but retained their significance.

140



141 **2.3 NEE calculation**

142 We calculated NEE from GPP and ER as follows (IPCC, 2021) (Equation 6):

143  $NEE = ER - GPP$  (6)

144 GHG exchange was calculated for each chamber following Equation 7.

145  $GHG\ exchange = CH_4 \cdot GWP_{CH_4} + N_2O \cdot GWP_{N_2O} + NEE$ , where: (7)

146  $GHG\ exchange$  was the greenhouse gas exchange in CO<sub>2</sub> equivalents (CO<sub>2</sub>eq),

147  $CH_4$  was the field-observed methane flux, mg CH<sub>4</sub> m<sup>-2</sup> h<sup>-1</sup>,

148  $GWP_{CH_4}$  was 28 CO<sub>2</sub>eq, the 100-year global warming potential of CH<sub>4</sub> without climate-carbon  
149 feedbacks (IPCC, 2021),

150  $N_2O$  was the field-observed nitrous oxide flux, mg N<sub>2</sub>O m<sup>-2</sup> h<sup>-1</sup>,

151  $GWP_{N_2O}$  was 265 CO<sub>2</sub>eq, the 100-year global warming potential of N<sub>2</sub>O without climate-carbon  
152 feedbacks (IPCC, 2021), and NEE was the net ecosystem exchange of CO<sub>2</sub> (Equation 6).

153 We considered carbon, N<sub>2</sub>O and CH<sub>4</sub> runoff as insignificant (Swails et al., in press) although  
154 they may evade in drained peatlands (Wilson et al., 2016, Taillardat et al., 2022, Nishida et al.,  
155 2023).

156 **2.4 Laboratory inorganic chemical and soil physical analyses**

157 The homogenised samples were divided into subsamples for physical-chemical analyses and  
158 DNA extraction. Plant-available phosphorus (P, NH<sub>4</sub>-lactate extractable) was determined on a  
159 FiaStar5000 flow-injection analyser. Plant-available potassium (K) was determined from the  
160 same solution by the flame-photometric method and plant-available magnesium (Mg) was  
161 determined from a 100mL NH<sub>4</sub>-acetate solution with a titanium-yellow reagent on the flow-  
162 injection analyser. Plant-available calcium (Ca) was analysed using the same solution by a  
163 flame-photometrical method. Soil pH was determined using a 1N KCl solution; soil NH<sub>4</sub> and  
164 NO<sub>3</sub> were determined on a 2M KCl extract of soil by flow-injection analysis (APHA, 2005).  
165 Total N and C contents of oven-dry samples were determined by a dry-combustion method on  
166 a varioMAX CNS elemental analyser (Elementar Analysensysteme GmbH, Germany).  
167 Organic matter content of dry matter was determined by loss on ignition (McLaren and  
168 Cameron, 2012). We determined SWC from gravimetric water content (GWC), dry matter  
169 content and empirically established bulk densities of mineral and organic matter fractions (Pärn  
170 et al., 2018) and calibrated them with field measurements using a handheld GS3 sensor  
171 connected to a ProCheck handheld reader (Decagon Devices, Pullman, WA, USA) and a Teros  
172 12 sensor (METER Group, USA).

173 **2.5 Correlation analysis of GHG against environmental factors**

174 We calculated a correlation matrix between our individual GHG fluxes and their total  
175 CO<sub>2</sub>eq exchange values, environmental factors, relative abundances of functional groups of  
176 microbes and ratios between them. We used linear and non-parametric GAM models applying  
177 variable smoothness factors (starting from minimal smoothness: k=3; Pärn et al., 2018). We  
178 assessed normality of our data using visual approaches and the Shapiro-Wilk test. Where  
179 necessary, we log-transformed the values. For the GHG flux rates, we considered the following  
180 environmental predictor variables: soil and water temperature, water table, volumetric SWC,  
181 soil chemistry (pH, total C%, organic matter, total N%, C:N ratio, ammonium, nitrate, calcium,  
182 magnesium, potassium and phosphorus), water oxygen content. We calculated Pearson  
183 correlations using the R programming language (*stats* and *mgcv* packages). We reported  
184 correlations with a significance level of p=0.05.

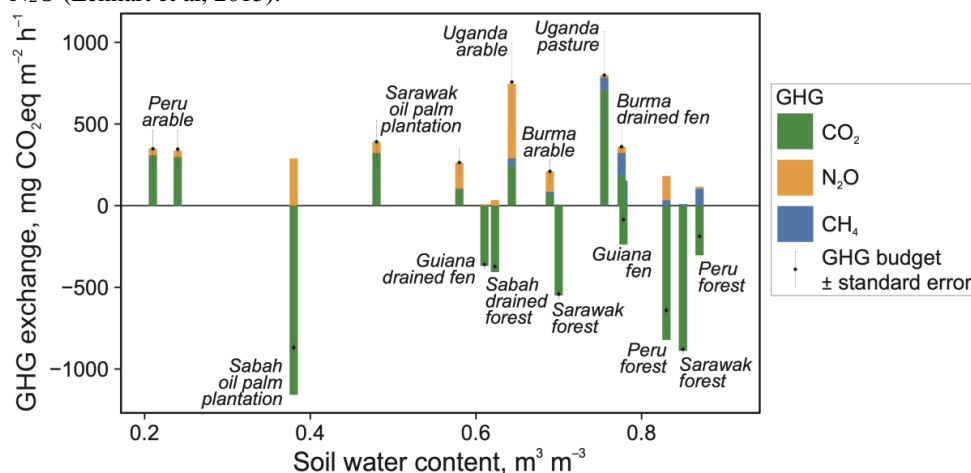
185

186

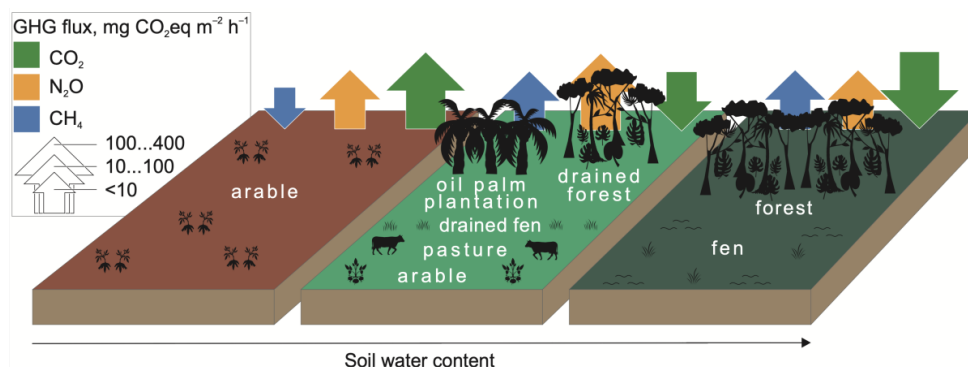


187 **3 Results and Discussion**

188 CO<sub>2</sub> dominated the GHG budgets with overall net ecosystem uptake 160 mg m<sup>-2</sup> h<sup>-1</sup> (Figs. 2,  
 189 3). The wet (SWC >0.8 m<sup>3</sup> m<sup>-3</sup>) peat swamp forests and the drained Sabah oil palm  
 190 plantation were the large net CO<sub>2</sub> and thus overall GHG sinks. This corroborates the  
 191 conclusion of the IPCC (2021) and several other global studies on CO<sub>2</sub> as the predominant  
 192 GHG, with CH<sub>4</sub> as a minor component. The rest of dry and moderately drained peatlands  
 193 were evenly distributed between sinks and sources of CO<sub>2</sub>. (Fig. 2). N<sub>2</sub>O emission contributed  
 194 overall 90 mg CO<sub>2</sub>-equivalent m<sup>-2</sup> h<sup>-1</sup>. The moderately drained peatlands (SWC 0.35–0.70 m<sup>3</sup>  
 195 m<sup>-3</sup>) contributed the largest N<sub>2</sub>O fluxes. The peak N<sub>2</sub>O emissions in moderately drained peat  
 196 soils is well known (Pärn et al. 2018). At the two extremes of the SWC spectrum, the dry  
 197 Peruvian arable field (<0.25 m<sup>3</sup> m<sup>-3</sup> SWC) and the wet but oxygenated ammonium-rich  
 198 Peruvian swamp forest emitted considerable amounts of N<sub>2</sub>O – 41 and 90 mg CO<sub>2</sub>-equivalent  
 199 m<sup>-2</sup> h<sup>-1</sup>, respectively. Our measured N<sub>2</sub>O emissions contrasted the earlier-reported negligible  
 200 emissions from a Peruvian palm peat swamp forest (Teh et al. 2017) and were relatively high  
 201 compared to the average 31 ± 22 μg N<sub>2</sub>O-N m<sup>-2</sup> h<sup>-1</sup> (average ± standard deviation across  
 202 studies) from the 410 ± 120 mg dry kg<sup>-1</sup> soil NH<sub>4</sub><sup>+</sup>-N in Southeast Asian wetland forests (van  
 203 Lent et al. 2015). Our measured fluxes were higher than model-predicted emissions of 21 μg  
 204 N<sub>2</sub>O-N m<sup>-2</sup> h<sup>-1</sup> for the Amazon Basin (Guilhen et al. 2020). Our N<sub>2</sub>O emissions were log-log  
 205 linear positively related to soil nitrate content and formed a unimodal relationship with SWC  
 206 (Pärn et al., 2018). However, it has been observed that a large part of the soil N<sub>2</sub>O never  
 207 leaves the forest canopy space (Mander et al., 2021), either due to physical processes or the  
 208 canopy microbiome (van Groningen et al., 2015, Guerreri et al., 2021). Alternatively,  
 209 nitrogen-fixing cryptogamic covers on forest canopy surfaces can be additional sources of  
 210 N<sub>2</sub>O (Lenhart et al, 2015).



211 Fig. 2. GHG exchange in peatland sites along the soil water content gradient. Breakdown of  
 212 GHG budgets into individual fluxes along soil water content gradient. Site average (bars for  
 213 individual gases and points for total GHG budget) and standard error (whiskers) are shown.  
 214 Data from Pärn et al. (2018, 2023 and partly unpublished (Sarawak)).  
 215



216  
217 Fig. 3. GHG fluxes and land use along the soil water content gradient. Data from Pärn et al.  
218 (2018, 2023 and partly unpublished (Sarawak)).  
219

220 Surprisingly for peatlands, CH<sub>4</sub> comprised only a minor share of the GHG budgets – on  
221 average, 36 mg CO<sub>2</sub>-equivalent m<sup>-2</sup> h<sup>-1</sup> across the full soil moisture spectrum. The emissions  
222 followed SWC in a GAM function that peaked at 0.8 m<sup>3</sup> m<sup>-3</sup> SWC (k=6; R<sup>2</sup>= 0.51), which  
223 corresponded to anoxic conditions created by stagnant ground-level water table, and decreased  
224 again towards the fully submerged peatlands under mobile water. Turetsky and colleagues  
225 (2014) have shown a similar distribution in extratropical peatlands. Accordingly, our wetter  
226 peat soils (>0.76 m<sup>3</sup> m<sup>-3</sup> SWC) produced practically all the CH<sub>4</sub> while the drier peat soils (<0.6  
227 m<sup>3</sup> m<sup>-3</sup> SWC) emitted CH<sub>4</sub> negligibly (<4 mg CO<sub>2</sub>-equivalent m<sup>-2</sup> h<sup>-1</sup>) or took it up (Figs. 2, 3).  
228 Our observed CH<sub>4</sub> fluxes were similar to reports from Brazilian swamp forest soils (*igapo* and  
229 *varzea*; Pangala et al. 2017). The moderate explanatory power of our GAM model can be  
230 explained by the intrinsic confinement of CH<sub>4</sub> emissions to individual emission hot spots  
231 (Becker et al., 2008). However, as CH<sub>4</sub> was a minor component of GHG exchange (Fig. 2), the  
232 >40% uncertainty in CH<sub>4</sub> flux estimates does not translate into large uncertainty in GHG  
233 exchange across the tropical belt. Permanently anoxic environments normally show high CH<sub>4</sub>  
234 production (Turetsky et al., 2014, IPCC, 2021). The low share of CH<sub>4</sub> in the GHG exchange of  
235 our wet peatlands suggests indirect human influence through a legacy of climatic drying. In the  
236 forests, however, tree trunks and leaves can conduct or produce additional CH<sub>4</sub> into the  
237 atmosphere (Keppler et al., 2006; Pangala et al., 2017; Soosaar et al., 2022).

#### 238 4 Conclusions

239 The tropical peatlands showed high GHG turnover rates, varying between sinks and sources of  
240 CO<sub>2</sub>. N<sub>2</sub>O was the second most important part of the GHG budget, particularly in the nitrogen-  
241 rich peatlands. The resulting high GHG emissions demand close monitoring of soil moisture  
242 and nitrogen in tropical peatlands. We highlight the need to consider not only carbon but all  
243 three main greenhouse gases (CO<sub>2</sub>, N<sub>2</sub>O and CH<sub>4</sub>) in tropical peatland GHG budgets.  
244 Management of tropical peatlands should be aware of the impact changes in soil moisture and  
245 nitrogen availability have on GHG emissions. Conservation of swamp forests is the safest way  
246 to keep up the carbon uptake and minimise the GHG emissions. Future impacts of global  
247 change on GHG exchange and the state of peatland ecosystems will be accordingly determined  
248 by drying and mineralisation of peat. Future studies will have to account for the production and  
249 consumption rates of CH<sub>4</sub> as well as N<sub>2</sub>O in all parts of the soil–tree–atmosphere continuum.

#### 250 Data Availability

251 The study is mostly based on data published in Pärn et al., (2018, 2023). Additional source data  
252 (CO<sub>2</sub> and CH<sub>4</sub> fluxes and unpublished data from Sarawak) are provided with this paper.

#### 253 Author Contribution



254 Jaan Pärn and Ülo Mander designed and managed the study. Jaan Pärn, Mikk Espenberg, Kaido  
255 Soosaar, Kuno Kasak, Thomas Schindler, Lulie Melling, Lizardo Fachín, Reti Ranniku and  
256 Ülo Mander planned and participated in the field sampling. Sandeep Thayamkottu extracted  
257 the remotely sensed GPP data. Jaan Pärn analysed the data and wrote the paper with conceptual  
258 input from Ülo Mander, Mikk Espenberg, Kaido Soosaar, Sandeep Thayamkotu and Kristina  
259 Sohar.

#### 260 **Acknowledgements**

261 The study was supported by the Ministry of Education and Science of Estonia (SF0180127s08  
262 grant), the Estonian Research Council (IUT2-16, PRG-352, PRG-609, PRG2032, MOBERC20  
263 and MOBERC44), European Research Council (ERC) under the grant agreement No  
264 101096403 (MLTOM23415R), European Commission through the HORIZON-WIDERA  
265 ‘Living Labs for Wetland Forest Research’ Twinning project No 101079192 and the European  
266 Regional Development Fund (Centres of Excellence ENVIRON, grant number TK-107, and  
267 EcolChange, grant number TK-131), and the European Social Fund (Doctoral School of Earth  
268 Sciences and Ecology). We are grateful to Dr. G. Gabiri, Dr. J.B. Gallagher, Dr. J. Järveoja, C.  
269 Luswata, Dr. M. Maddison, Dr. T. Pae, A.A. Rabar, Dr. F. Sangok, Dr. M. Tenywa, G.X.  
270 Wong, S.S. Zaw, W. A. Muñoz, J. L. Jibaja Aspajo, R. I. Negron-Juarez, J. Rengifo, D. J.  
271 Garay Dinis, A. G. Arista Oversluijs, M. C. Ávila Fucos, R. Chávez Vásquez, R. Huaje  
272 Wampuch, E. Peas García, S. Cordova Horna, T. Pacheco Gómez, J. D. Urquiza Muñoz, R.  
273 Tello Espinoza for help with site selection and field investigation.

#### 274 **Competing Interest**

275 The authors declare that they have no conflict of interest.

276

#### 277 **References**

278

279 APHA: Standard Methods for the Examination of Water and Wastewater. 21st Edition,  
280 American Public Health Association/American Water Works Association/Water Environment  
281 Federation, Washington DC, 2005.

282

283 Bahram, M., Espenberg, M., Pärn, J., ... and Mander, Ü.: Structure and function of the soil  
284 microbiome underlying N<sub>2</sub>O emissions from global wetlands. *Nature Communications* 13,  
285 1430, 2022.

286

287 Becker, T. et al.: Do we miss the hot spots? – The use of very high resolution aerial photographs  
288 to quantify carbon fluxes in peatlands. *Biogeosciences* 5, 1387–1393, 2008.

289

290 Espenberg, M., Truu, M., Mander, Ü., Kasak, K., Nölvak, H., Ligi, T., Oopkaup, K., Maddison,  
291 M. and Truu, J.: Differences in microbial community structure and nitrogen cycling in natural  
292 and drained tropical peatland soils. *Scientific Reports*, 8:4742, 2018.

293

294 Friedl, M. and Sulla-Menashe, D. MCD12Q1 MODIS/Terra+Aqua Land Cover Type Yearly  
295 L3 Global 500m SIN Grid V006. NASA EOSDIS Land Processes DAAC, 2020.

296

297 Frohking, S. and Roulet, N.T.: Holocene radiative forcing impact of northern peatland carbon  
298 accumulation and methane emissions. *Global Change Biology*, 13:1079-1088, 2007.

299

300 Griffis, T.J., Roman, D.T., Wood, J.D., Deventer, J., Fachin, L., Rengifo, J., Del Castillo, D.,  
301 Lilleskov, E., Kolka, R., Chimner, R.A., del Aguila-Pasquel, J., Wayson, C., Hergoualc'h, K.,  
302 Baker, J.M., Cadillo-Quiroz, H. and Ricciuto, D.M.: Hydrometeorological sensitivities of net



- 303 ecosystem carbon dioxide and methane exchange of an Amazonian palm swamp peatland.  
304 *Agricultural and Forest Meteorology*, 295:108167, 2020.  
305
- 306 van Groenigen, J. W., Huygens, D., Boeckx, P., Kuyper, Th. W., Lubbers, I. M., Rütting, T.,  
307 and Groffman, P. M.: The soil N cycle: new insights and key challenges. *SOIL*, 1, 235–256,  
308 2015.  
309
- 310 Guerrieri, R., Templer, P. and Magnani, F.: Canopy Exchange and Modification of Nitrogen  
311 Fluxes in Forest Ecosystems. *Current Forestry Reports*, 7, 115–137, 2021.  
312
- 313 Guilhen, J., Al Bitar, A., Sauvage, S., Parrens, M., Martinez, J.M., Abril, G., Moreira-Turcq,  
314 P. and Sánchez-Pérez, J.M.: Denitrification and associated nitrous oxide and carbon dioxide  
315 emissions from the Amazonian wetlands. *Biogeosciences*, 17:4297-4311, 2020.  
316
- 317 Hadi, A., Inubushi, K., Purnomo, E., Razie, F., Yamakawa, K., and Tsuruta, H.: Effect of land-  
318 use changes on nitrous oxide (N<sub>2</sub>O) emission from tropical peatlands. *Chemosphere-Global  
319 Change Science*, 2(3-4), 347-358, 2000.  
320
- 321 Hergoualc’h, K., Dezzeo, N., Verchot, L.V., Martius, C., van Lent, J., del Aguila-Pasquel, J.  
322 and López Gonzales, M.: Spatial and temporal variability of soil N<sub>2</sub>O and CH<sub>4</sub> fluxes along a  
323 degradation gradient in a palm swamp peat forest in the Peruvian Amazon. *Global Change  
324 Biology*, 26(12), 7198-7216, 2020.  
325
- 326 Hu, H.-W., Chen, D. and He, J.-Z.: Microbial regulation of terrestrial nitrous oxide formation:  
327 understanding the biological pathways for prediction of emission rates. *FEMS Microbiology  
328 Reviews*, 39:729-749, 2015.  
329
- 330 IPCC: *Climate Change 2021: The Physical Science Basis. Contribution of Working Group I to  
331 the Sixth Assessment Report of the Intergovernmental Panel on Climate Change* [Masson-  
332 Delmotte, V., P. Zhai, A. Pirani, S. L. Connors, C. Péan, S. Berger, N. Caud, Y. Chen, L.  
333 Goldfarb, M. I. Gomis, M. Huang, K. Leitzell, E. Lonnoy, J. B. R. Matthews, T. K. Maycock,  
334 T. Waterfield, O. Yelekçi, R. Yu and B. Zhou (eds.)]. Cambridge University Press, 2021.  
335
- 336 Jassey, V.E.J., Reczuga, M.K., Zielińska, M., Słowińska, S., Robroek, B.J.M., Mariotte, P.,  
337 Seppey, C.V.W., Lara, E., Barabach, J., Słowiński, M., Bragazza, L., Chojnicki, B.H.,  
338 Lamentowicz, M., Mitchell, E.A.D. and Buttler, A.: Tipping point effect in plant–fungal  
339 interactions under severe drought causes abrupt rise in peatland ecosystem respiration. *Global  
340 Change Biology*, 24:972– 986, 2021.  
341
- 342 Jauhainen, J., Silvennoinen, H., Hämäläinen, R., Kusin, K., Limin, S., Raison, R.J. and  
343 Vasander, H.: Nitrous oxide fluxes from tropical peat with different disturbance history and  
344 management. *Biogeosciences*, 9:1337-1350, 2012.  
345
- 346 Karhu, K., Auffret, M. D., Dungait, J. A. J., Hopkins, D. W., Prosser, J. I., Singh, B. K., Subke,  
347 J.-A., Wookey, P. A., Ågren, G. I., Sebastià, M.-T., Gouriveau, F., Bergkvist, G., Meir, P.,  
348 Nottingham, A. T., Salinas, N., and Hartley, I. P.: Temperature sensitivity of soil respiration  
349 rates enhanced by microbial community response, *Nature*, 513, 81-84, 2014.  
350
- 351 Keppler, F., Hamilton, J., Braß, M. et al.: Methane emissions from terrestrial plants under  
352 aerobic conditions. *Nature*, 439, 187–191, 2006.





- 353  
354 Leifeld, J. and Menichetti, L.: The underappreciated potential of peatlands in global climate  
355 change mitigation strategies. *Nature Communications*, 9:1071, 2018.  
356  
357 Lenhart, K., Weber, B., Elbert, W., Steinkamp, J., Clough, T., Crutzen, P., Pöschl, U. and  
358 Keppler, F.: Nitrous oxide and methane emissions from cryptogamic covers. *Global Change*  
359 *Biology*, 21:3889-3900, 2015.  
360  
361 Lent, J. van, Hergoualc'h, K. and Verchot, L.V., Reviews and syntheses: Soil N<sub>2</sub>O and NO  
362 emissions from land use and land-use change in the tropics and subtropics: a meta-analysis.  
363 *Biogeosciences*, 12:7299-7313, 2015.  
364  
365 Lent, J. van, Hergoualc'h, K., Verchot, L., Oenema, O. and Groenigen, J.W. van: Greenhouse  
366 gas emissions along a peat swamp forest degradation gradient in the Peruvian Amazon: soil  
367 moisture and palm roots effects. *Mitigation and Adaptation Strategies for Global Change*,  
368 24:625-643, 2019.  
369  
370 Li, C., Frohling, S. and Frohling, T.A.: A model of nitrous oxide evolution from soil driven by  
371 rainfall events: 1. Model structure and sensitivity. *Journal of Geophysical Research:*  
372 *Atmospheres*, 97:9759-9776, 1992.  
373  
374 Lienggaard, L., Figueiredo, V., Markfoged, R., Revsbech, N.P., Nielsen, L.P., Prast, A.E. and  
375 Kühl, M.: Hot moments of N<sub>2</sub>O transformation and emission in tropical soils from the Pantanal  
376 and the Amazon (Brazil). *Soil Biology and Biochemistry*, 75:26-36, 2014.  
377  
378 Lilleskov, E., McCullough, K., Hergoualc'h, K., del Castillo Torres, D., Chimner, R.,  
379 Murdiyarmo, D., Kolka, R., Bourgeau-Chavez, L., Hribljan, J., del Aguila Pasquel, J. and  
380 Wayson, C.: Is Indonesian peatland loss a cautionary tale for Peru? A two-country comparison  
381 of the magnitude and causes of tropical peatland degradation. *Mitigation and Adaptation*  
382 *Strategies for Global Change*, 24:591-623, 2019.  
383  
384 Loisel, J., Gallego-Sala, A.V., Amesbury, M.J., Magnan, G., Anshari, G., Beilman, D.W., ...  
385 and Wu, J.: Expert assessment of future vulnerability of the global peatland carbon sink. *Nature*  
386 *Climate Change*, 11:70-77, 2021.  
387  
388 Mander, Ü., Krasnova, A., Escuer-Gatius, J., Espenberg, M., Schindler, T., Machacova, K.,  
389 Pärn, J. ... and Soosaar, K.: Forest canopy mitigates soil N<sub>2</sub>O emission during hot moments.  
390 *npj Climate and Atmospheric Science* 4, 39, 2021.  
391  
392 McLaren, R. G. and Cameron, K. C.: *Soil Science: Sustainable Production and Environmental*  
393 *Protection*. Oxford University Press, Wallingford, UK, 2012.  
394  
395 Melillo, J.M., Steudler, P.A., Feigl, B.J., Neill, C., Garcia, D., Piccolo, M.C., Cerri, C.C. and  
396 Tian, H.: Nitrous oxide emissions from forests and pastures of various ages in the Brazilian  
397 Amazon. *Journal of Geophysical Research: Atmospheres*, 106:34179-34188, 2001.  
398  
399 Melling, L., Hatano, R., Goh, K.J.: Soil CO<sub>2</sub> flux from three ecosystems in tropical peatland of  
400 Sarawak, Malaysia. *Tellus B: Chemical and Physical Meteorology* 57(1): 1-11, 2005a.  
401  
402 Melling, L., Hatano, R., Goh, K.J.: Methane fluxes from three ecosystems in tropical



- 403 peatland of Sarawak, Malaysia. *Soil Biology and Biochemistry* 37(8): 1445-1453, 2005b.  
404  
405 Melling, L., Hatano, R., Goh, K.J.: Nitrous oxide emissions from three ecosystems in tropical  
406 peatland of Sarawak, Malaysia. *Soil Science and Plant Nutrition* 53(6): 792-805, 2007.  
407  
408 Monteith, J. L. Solar radiation and productivity in tropical ecosystems. *Journal of Applied*  
409 *Ecology*, 9, 747–766, 1972.  
410  
411 Nishina, K., Melling, L., Toyoda, S., Itoh, M., Terajima, K., Waili, J. W., ... and Onodera, T.:  
412 Dissolved N<sub>2</sub>O concentrations in oil palm plantation drainage in a peat swamp of Malaysia.  
413 *Science of The Total Environment*, 872, 162062, 2023.  
414  
415 Pangala, S.R., Enrich-Prast, A., Basso, L.S., Peixoto, R.B., Bastviken, D., Hornibrook, E.R.C.,  
416 Gatti, L.V., Marotta, H., Calazans, L.S.B., Sakuragui, C.M., Bastos, W.R., Malm, O., Gloor,  
417 E., Miller, J.B. and Gauci, V.: Large emissions from floodplain trees close the Amazon  
418 methane budget. *Nature*, 552:230-234, 2017.  
419  
420 Pärn, J., Verhoeven, J. T. A., Butterbach-Bahl, K., Dise, N. B., Ullah, S., Aasa, A., Egorov, S.,  
421 Espenberg, M., Järveoja, J., Jauhiainen, J., Kasak, K., Klemetsson, L., Kull, A., Laggoun-  
422 Défarge, F., Lapshina, E. D., Lohila, A., Löhmus, K., Maddison, M., Mitsch, W. J., Müller, C.,  
423 Niinemets, Ü., Osborne, B., Pae, T., Salm, J.-O., Sgouridis, F., Sohar, K., Soosaar, K., Storey,  
424 K., Teemusk, A., Tenywa, M. M., Tournebize, J., Truu, J., Veber, G., Villa, J. A., Zaw, S. S.,  
425 and Mander, Ü.: Nitrogen-rich organic soils under warm well-drained conditions are global  
426 nitrous oxide emission hotspots, *Nature Communications*, 9, 1135, 2018.  
427  
428 Pärn, J., Soosaar, K., Schindler, T., Machacova, K., Muñoz, W. A., Fachín, L., ... and Mander,  
429 Ü.: Effects of water table fluctuation on greenhouse gas emissions from wetland soils in the  
430 Peruvian Amazon. *Wetlands*, 43(6), 62, 2023.  
431  
432 Ribeiro, K., Pacheco, F.S., Ferreira, J.W., de Sousa-Neto, E.R., Hastie, A., Krieger Filho, G.C.,  
433 Alvalá, P.C., Forti, M.C. and Ometto, J.P.: Tropical peatlands and their contribution to the  
434 global carbon cycle and climate change. *Global Change Biology*, 27: 489–505, 2021.  
435  
436 Ricaud, P., Attié, J. L., Teyssèdre, H., El Amraoui, L., Peuch, V. H., Matricardi, M., and  
437 Schluessel, P.: Equatorial total column of nitrous oxide as measured by IASI on MetOp-A:  
438 implications for transport processes, *Atmospheric Chemistry and Physics*, 9, 3947-3956, 2009.  
439  
440 Roucoux, K. H., Lawson, I. T., Jones, T. D., Baker, T. R., Coronado, E. N. H., Gosling, W.  
441 D., and Lähteenoja, O.: Vegetation development in an Amazonian peatland, *Palaeogeogr.,*  
442 *Palaeoclimatol., Palaeoecol.*, 374, 242-255, 2013.  
443  
444 Rubol, S., Silver, W. L., and Bellin, A.: Hydrologic control on redox and nitrogen dynamics in  
445 a peatland soil, *Science of the Total Environment*, 432, 37-46, 2012.  
446  
447 Running, S., Q. Mu and M. Zhao. MOD17A2H MODIS/Terra Gross Primary Productivity 8-  
448 Day L4 Global 500m SIN Grid V006., distributed by NASA EOSDIS Land Processes DAAC,  
449 2015.  
450



- 451 Ruwaimana, M., Anshari, G. Z., Silva, L. C., and Gavin, D. G.: The oldest extant tropical  
452 peatland in the world: a major carbon reservoir for at least 47 000 years, *Environmental*  
453 *Research Letters*, 15, 114027, 2020.
- 454  
455 Ruzicka, J. and Hansen, E. H.: *Flow Injection Analysis*, J. Wiley & Sons, New York, 1981.  
456
- 457 Rydin H and Jeglum JK (2013) *The Biology of Peatlands* (2nd ed.). Oxford Academic Press.  
458
- 459 Sellers, P. J. Canopy reflectance, photosynthesis, and transpiration, II. The role of biophysics  
460 in the linearity of their interdependence. *Remote Sens. Envir.* 21, 143–183 (1987).  
461
- 462 Soosaar K., Schindler T., Machacova K., Pärn J., Fachín-Malaverri LM, Rengifo-Marin, JE, ...  
463 and Mander Ü (2022) High methane emission from palm stems and nitrous oxide emission  
464 from the soil in a peruvian Amazon peat swamp forest. *Frontiers in Forests and Global Change*,  
465 36  
466
- 467 Stocker, B.D., Zscheischler, J., Keenan, T.F. et al. Drought impacts on terrestrial primary  
468 production underestimated by satellite monitoring. *Nat. Geosci.* 12, 264–270 (2019).  
469
- 470 Swails, E., Frohling, S., Deng, J., Hergoualc’h, K. Degradation increases peat greenhouse gas  
471 emissions in undrained tropical peat swamp forests. *Biogeochemistry* (accepted): in press.  
472
- 473 Taillardat, P., Bodmer, P., Deblois, C. P., Ponçot, A., Prijac, A., Riahi, K., et al.: Carbon  
474 dioxide and methane dynamics in a peatland headwater stream: Origins, processes and  
475 implications. *Journal of Geophysical Research: Biogeosciences*, 127, e2022JG006855, 2022.  
476
- 477 Teh, Y. A., Wayne, M., Berrio, J.-C., Boom, A., and Page, S. E.: Seasonal variability in  
478 methane and nitrous oxide fluxes from tropical peatlands in the western Amazon basin,  
479 *Biogeosciences*, 2017.  
480
- 481 Thompson, R. L., Lassaletta, L., Patra, P. K., Wilson, C., Wells, K. C., Gressent, A., Koffi, E.  
482 N., Chipperfield, M. P., Winiwarter, W., Davidson, E. A., Tian, H., and Canadell, J. G.:  
483 Acceleration of global N<sub>2</sub>O emissions seen from two decades of atmospheric inversion, *Nature*  
484 *Climate Change*, 9, 993-998, 2019.  
485
- 486 Turetsky, M.R., Kotowska, A., Bubier, J., Dise, N.B., Crill, P., Hornibrook, E.R.C.,  
487 Minkinen, K., Moore, T.R., Myers-Smith, I.H., Nykänen, H., Olefeldt, D., Rinne, J., Saarnio,  
488 S., Shurpali, N., Tuittila, E.-S., Waddington, J.M., White, J.R., Wickland, K.P. and Wilmking,  
489 M.: A synthesis of methane emissions from 71 northern, temperate, and subtropical wetlands.  
490 *Global Change Biology*, 20:2183-2197, 2014.  
491
- 492 Turetsky, M. R., Bencotter, B., Page, S., Rein, G., van der Werf, G. R., and Watts, A.: Global  
493 vulnerability of peatlands to fire and carbon loss, *Nature Geoscience*, 8, 11-14, 2015.  
494
- 495 Wilson, D., Blain, D., Couwenberg, J., Evans, C. D., Murdiyarso, D., Page, S., ... and  
496 Tuittila, E. S.: Greenhouse gas emission factors associated with rewetting of organic soils.  
497 *Mires and Peat*, 17, Article 04, 2016.  
498



499 Zhao, J., Weldon, S., Barthelmes, A., Swails, E., Hergoualc'h, K., Mander, Ü., ... and  
500 Campbell, D. I.: Global observation gaps of peatland greenhouse gas balances: needs and  
501 obstacles. *Biogeochemistry*, 2023.